J Solid State Electrochem (2009) 13:1259–1265
DOI 10.1007/s10008-008-0660-x

ORIGINAL PAPER

# Electrocatalytic activities of binary and ternary composite electrodes of Pd, nanocarbon and Ni for electro-oxidation of methanol in alkaline medium

**R. N. Singh · A. Singh · Anindita**

Received: 10 July 2008 / Revised: 21 August 2008 / Accepted: 24 August 2008 / Published online: 6 September 2008


**Abstract** Films of binary and ternary composites of Pd, nanocarbon (C), and Ni are obtained on glassy carbon electrodes and investigated as electrocatalysts for methanol oxidation (MOR) in alkaline medium. Results show that among the electrocatalysts investigated, the apparent electrocatalytic activity of the Pd-0.5%C electrode is the greatest and that it decreases with increasing percentage of C in the composite. The Pd-0.5%C composite electrode has approximately two times higher activity than that of Pd electrode for MOR under similar experimental conditions. Introduction of Ni (1–2%) into the active Pd-0.5%C catalyst somewhat declines the apparent electrocatalytic activity of the electrode. The onset potential for MOR is observed to be the greatest negative at the Pd-0.5%C composite electrode, which gets shifted towards noble side by 80–100 mV with addition of Ni (1–2%).

**Keywords** Methanol oxidation · Composite films · Direct methanol fuel cells (DMFCs) · Electrocatalysis

## Introduction

Direct methanol fuel cells (DMFCs) are recognized to be a promising power source for portable electronic devices and electric vehicles [1, 2]. However, these fuel cells suffer from two major problems, the relatively high overpotential for methanol electro-oxidation reaction and high methanol crossover through the membrane [3, 4]. To improve the kinetics of methanol oxidation (MOR), the Pt catalyst is, generally, alloyed with Ru and impregnated/deposited over conductive supports, such as carbon powder, carbon blacks, carbon nanofibers, carbon (single walled/double walled) nanotubes, and fullerene soot [5–7]. However, Pt-based anodes invariably undergo deactivation due to poisoning by the reaction intermediates, particularly CO in acid medium. It is therefore desired to develop low-cost non-platinum electrocatalysts with comparable or improved kinetics for anodic methanol/ethanol oxidation.

Many non-noble metals have recently been studied in alkaline media [8–12]. Among them, Pd is a suitable low-cost transition metal of high catalytic activity towards methanol oxidation [13–15] and about 50 times more abundant in the earth than Pt [16]. Recently, Masel et al. [17, 18] have disclosed that Pd and Pd/C catalysts can overcome the CO-poisoning effect and thereby yield high performance in DMFCs. Thus, Pd seems to be a promising anode in an alkaline DMFC. It is therefore of interest to improve the electrocatalytic activity of Pd catalysts towards methanol oxidation.

In recent years, efforts have been made [19–24] to improve the catalytic efficiency of Pd catalysts by suitable means. Lee [19] and Lee et al. [20] obtained carbon-nanomaterials-supported Pd nanoparticles by self-regulated reduction of surfactant; these novel catalysts exhibited high activity for $O_2$ reduction in 1 M $H_2SO_4$. Wang et al. [21] and Zhang and Li [22] have demonstrated that binary composites of Pd with $TiO_2$ nanotubes and C are much superior to that of pure Pd with respect to electrocatalysis vis-à-vis stability for methanol oxidation in acid medium. Zhang et al. [23] obtained well-dispersed Pd nanoparticles on the surface of vanadium oxide nanotubes ($VO_x$ NTs) through a simple reductive process and investigated them as electrocatalysts for MOR in alkaline medium. The new materials were found to exhibit an excellent electrocatalytic

R. N. Singh (✉) · A. Singh · Anindita
Chemistry Department, Science Faculty,
Banaras Hindu University,
Varanasi 221005, India
e-mail: rnsbhu@rediffmail.com

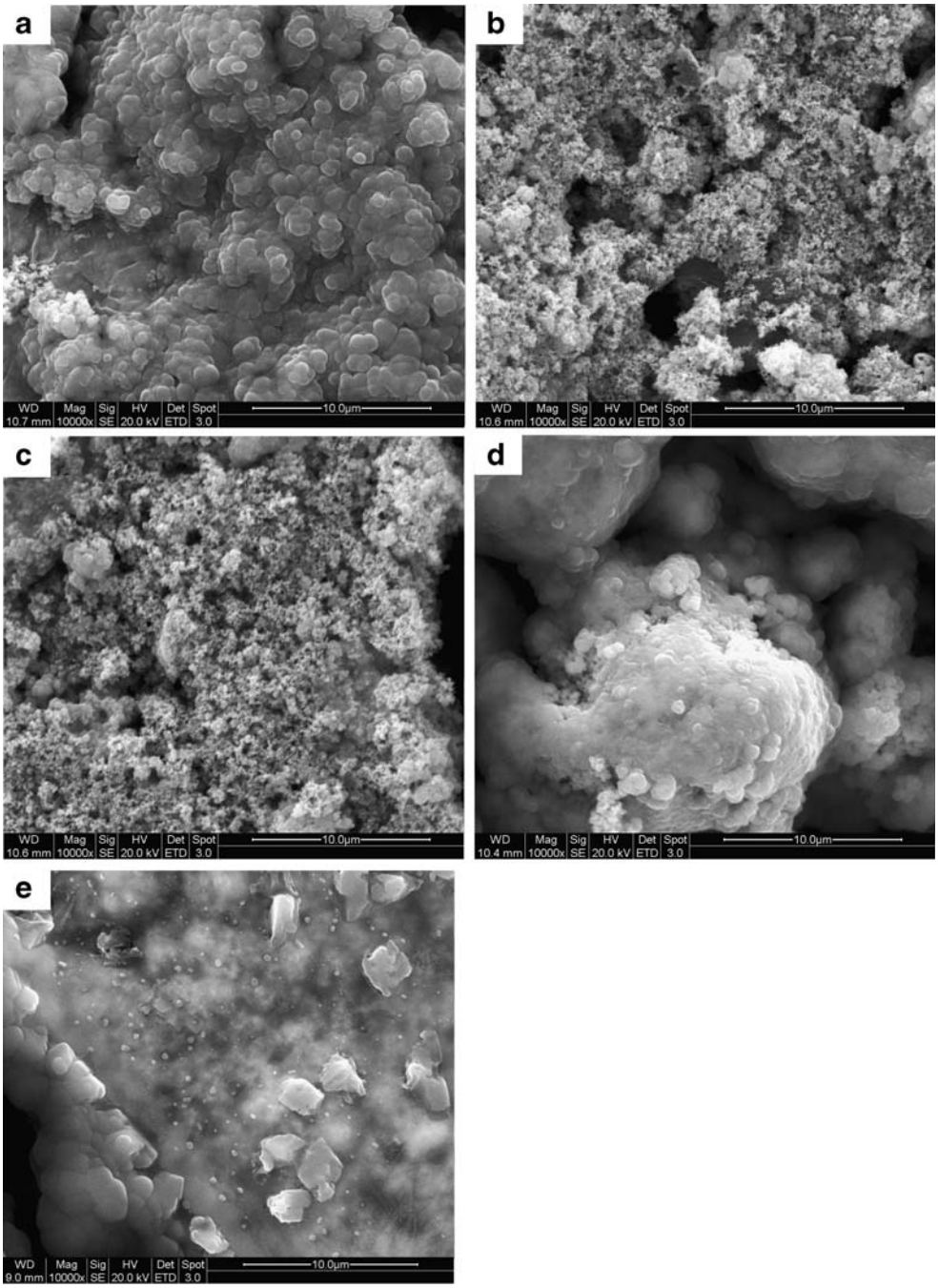


**Fig. 1** SEM pictures of films of Pd (**a**), Pd-0.5%C (**b**), Pd-0.5% C-1%Ni (**c**), Pd-2%C (**d**), and Pd-0.5%C-2%Ni (**e**) on glassy carbon

activity and good stability under alkaline condition. Shen et al. [24] observed that the presence of NiO into the Pd/C composite improves the electrocatalytic activity of the electrode considerably. The electrode with a weight ratio of Pd to NiO of 4:1 exhibited the highest electrocatalytic activity for methanol oxidation in alkaline medium.

We have obtained thin films of pure Pd and of binary composites of Pd and nanocarbon and ternary composites of Pd, nanocarbon, and Ni and investigated them as electrocatalysts for MOR in 1 M KOH at 298 K. Details of results of the investigation are presented in the present paper.

## Experimental

### Electrocatalyst preparation

Before use, the carbon nanopowder (Aldrich, 99+%) was activated by refluxing in concentrated $HNO_3$ for 5 h as described elsewhere [25]. Twenty milligrams of each catalyst, namely Pt, Pd, Pd–C, and Pd–C–Ni, was prepared. Pure metal catalyst Pt (or Pd) was obtained by dissolving required amount of $H_2PtCl_6{\cdot}6H_2O$ (Sigma-Aldrich, A.C.S. Reagent; or $PdCl_2$, anhydrous, Merck) in 5 ml acidified

double distilled water and subsequent reduction of metal ion by adding excess $NaBH_4$ (Sigma-Aldrich, 98%) solution under stirred condition. To obtain binary composites of Pd and C, the required amount of $PdCl_2$ in 5 ml acidified distilled water was dissolved and to this was added the required amount of activated carbon nanopowder, and the solution was stirred well. In order to carry out the complete reduction of the metal ions, the $NaBH_4$ solution was added in slightly excess under vigorously stirred condition. The addition of $NaBH_4$ solution was made in a dropwise manner. Similarly, ternary composites of Pd, C, and Ni were also prepared. $NiCl_2$ (Merck) was used as precursor for Ni. Each catalyst formed as a solid residue in the solution was centrifuged, repeatedly washed with double distilled water so as to remove $Cl^-$ ions, and finally dried overnight in a vacuum dessicator.

### Electrode preparation

The catalyst obtained in powder form was mixed with few milliliters of an ethanol (Merck)–water mixture and then ultrasonicated for 15 min so as to obtain an ink. To obtain the electrode, two to three drops of ink were dropped on to a pretreated glassy carbon plate through a syringe, dried, and then one drop of 1% Nafion solution (Alfa Aesar) was dropped over the dried catalyst layer to cover it. The catalyst electrodes, thus obtained, were finally irradiated with microwave (800 W) for 1 min. Prior to use as support for the catalyst, glassy carbon plates were first polished well on a micro cloth pad on a polishing machine with alumina powder and then dipped in 0.2 M $H_3PO_4$ solution for 5 min, degreased in acetone by ultrasonication, washed with distilled water, and dried. Electrical contact with the catalyst overlayer and electrode mounting were carried out as described elsewhere [26].

A scanning electron microscope (Quanta 200 FEI) was used to study the morphology of electrocatalysts as-obtained in the film form on glassy carbon (GC).

### Electrochemical studies

Electrochemical studies, namely, cyclic voltammetry, impedance spectroscopy, chronoamperometry, and Tafel polarization have been carried out in a three-electrode single-compartment Pyrex glass cell using an electrochemical impedance system (PARC, USA). A Pt foil (~8 $cm^2$) and an Hg/HgO/1 M KOH were used as auxiliary and reference electrodes, respectively. Cyclic voltammetry of each electrocatalyst has been carried out between −0.80 and +0.60 V versus Hg/HgO in 1 M KOH with and without containing methanol at 298 K. Before recording, the final voltammogram of each electrode was cycled for five runs at a scan rate of 50 mV $s^{-1}$in 1 M KOH. The anodic polarization curves ($E$ versus log $j$) were recorded using a run program with conditioning time=200 s, conditioning potential=−0.50 V, initial delay=pass, scan rate=0.2 mV $s^{-1}$, initial potential=−0.50 V, and IR interruption=10 s.

The study of electrochemical impedance spectroscopy (EIS) of electrodes in 1 M KOH+1 M $CH_3OH$ at a constant dc potential was carried out by recording EIS spectra over a frequency range of 0.5–2.5×$10^4$ Hz. The ac voltage amplitude of 10 mV was used in each measurement. Softwares used in impedance measurements and circuit analyses were ‘Power Sine’ and ‘ZSimpWin version 3.00.

All electrochemical experiments were performed in an Ar-deoxygenated 1 M KOH (GR Merck, 85%)+1 M $CH_3OH$ (GR Merck, 99.8%) at 298 K. The potential values mentioned in the text are given against the Hg/HgO/1 M KOH electrode only.

## Results and discussion

### Morphology

Figure 1 shows scanning electron microscopy (SEM) pictures of films of Pd, Pd-0.5%C, Pd-2%C, Pd-0.5%C-1%Ni, and Pd-0.5%C-2%Ni as-deposited on GC electrodes. These micrographs demonstrate significant influence of minor additions of C and Ni on the morphology of Pd. The surface of pure Pd film seems to be compact and granulated. The addition of 0.5% C to Pd makes the film highly porous and amorphous like. But a higher addition of C (2%) tends to change the morphology from amorphous to granular one. On the other hand, the presence of 1% Ni in the Pd-0.5%C composite does not seem to modify the morphology. But, 2% Ni addition changes the morphology from amorphous to a flat porous granular look.

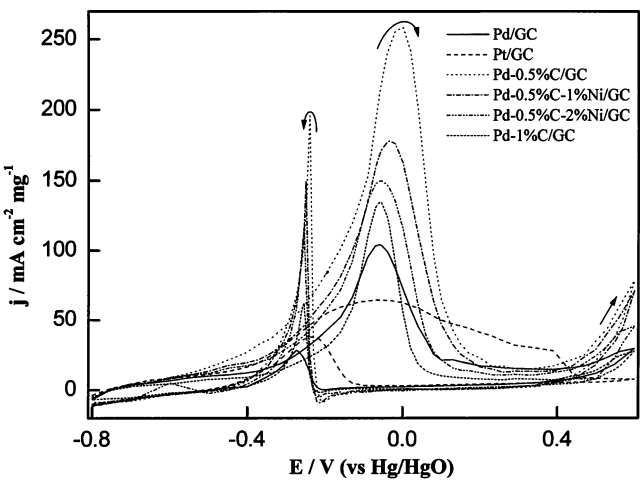


**Fig. 2** Cyclic voltammograms for Pt, Pd, Pd-C, and Pd-C-Ni electrodes in 1 M KOH+1 M $CH_3OH$ at 298 K

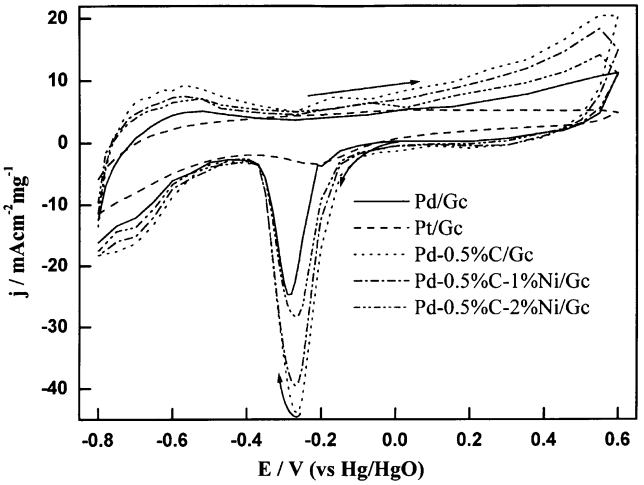


**Fig. 3** Cyclic voltammograms for Pt, Pd, Pd-C, and Pd-C-Ni electrodes in 1 M KOH at 298 K

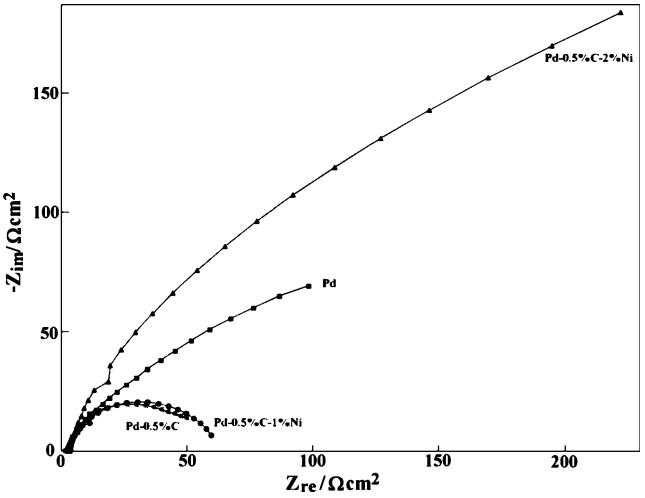


**Fig. 4** The Nyquist plots of electrocatalysts at $E$=−0.25 V in 1 M KOH+1 M $CH_3OH$ at 298 K; *square*, Pd; *asterisk*, Pd-0.5%C; *circle*, Pd-0.5%C-1%Ni; *triangle*, Pd-0.5%C-2%Ni

## Cyclic voltammetry

Figure 2 represents the cyclic voltammograms for the Pt/GC, Pd/GC, Pd-0.5%C/GC, Pd-0.5%C-1%Ni/GC, Pd-0.5%C-2%Ni/GC, and Pd-1%C/GC electrodes in 1 M KOH+1 M $CH_3OH$ at 298 K. In each case, the sweep rate is 50 mV $s^{-1}$ in the potential range of −0.80 to +0.60 V. The CV of the Pt/GC electrode, obtained under identical conditions, is given for the purpose of comparison. The cyclic voltammograms of these electrodes in 1 M KOH without containing methanol have also been recorded under identical conditions; these voltammograms look to be similar. Some representative voltammograms are shown in Fig. 3. By comparing the cyclic voltammograms in the absence of methanol, a methanol oxidation peak under anodic condition can be clearly observed in the cyclic voltammograms of all the electrocatalysts in 1 M KOH+1 M $CH_3OH$.

The methanol electro-oxidation on each electrode of the present investigation has been characterized by two well-defined anodic current peaks: one in the forward (i.e., anodic condition) and the other one in the reverse scan. In the forward scan, the oxidation peak is corresponding to the oxidation of freshly chemisorbed species coming from methanol adsorption. The oxidation peak in the reverse scan is primarily associated with removal of carbonaceous species not completely oxidized in the forward scan than the oxidation of freshly chemisorbed species [27–29 and references therein]. CV curves shown in Fig. 2 were analyzed for the onset potential ($E_{OP}$), current peaks, and current peak potentials for the MOR, and their values are shown in Table 1.

Table 1 shows that all the composite electrocatalysts have higher activity for MOR than the pure Pd (or Pt) electrode. Among the electrodes investigated, the composite film of Pd and 0.5% nanocarbon on glassy carbon exhibits the highest oxidation peak current density (during the forward scan), which is ~2.3 times higher than that observed on pure Pd film of the same loading. Further, with the addition of 0.5% nanocarbon in Pd, the peak potentials corresponding to both the forward and reverse scans get displaced towards noble direction by 50 mV (i.e., from −0.055 to −0.005 V) and 25 mV (i.e., from −0.265 to −0.240 V), respectively. It is

**Table 1** Results of the study of cyclic voltammetry of Pd, Pt, Pd-C, and Pd-C-Ni electrodes in 1 M KOH+1 M $CH_3OH$ at 298 K

| Electrode | Loading (mg $cm^{-2}$) | Geometrical area ($cm^2$) | Onset potential, $E_{OP}$ (mV) | Forward scan | | Reverse scan | |
|---|---|---|---|---|---|---|---|
| | | | | $j_P$ (mA $cm^{-2}$ $mg^{-1}$) | $E_P$ (mV) | $j_p$ (mA $cm^{-2}$ $mg^{-1}$) | $E_p$ (mV) |
| Pt | 0.20 | 0.45 | ~−425 | 61.88 | −75 | 29.69 | −230 |
| Pd | 0.18 | 0.50 | ~−375 | 111.11 | −55 | 38.89 | −265 |
| Pd-0.5%C | 0.15 | 0.50 | ~−510 | 258.67 | −5 | 196.0 | −240 |
| Pd-1.0%C | 0.2 | 0.60 | ~−405 | 140.58 | −55 | 61.83 | −255 |
| Pd-2.0%C | 0.18 | 0.50 | ~−390 | 129.89 | −45 | 101.67 | −245 |
| Pd-5.0%C | 0.19 | 0.48 | ~−355 | 125.44 | −75 | 55.48 | −255 |
| Pd-0.5%C-1.0%Ni | 0.15 | 0.52 | ~−430 | 177.95 | −35 | 149.23 | −250 |
| Pd-0.5%C-2.0%Ni | 0.14 | 0.54 | ~−400 | 152.12 | −60 | 116.40 | −255 |

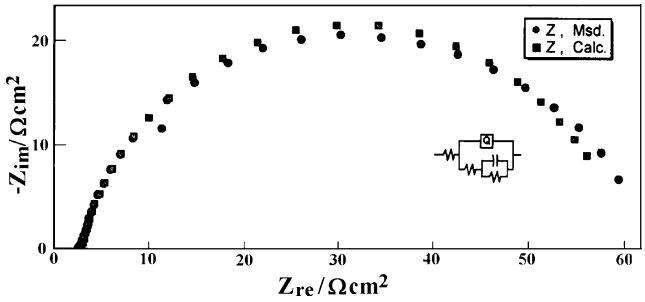


**Fig. 5** Typical Nyquist plots (experimental + simulated) for the Pd-0.5%C-1%Ni electrode from Fig. 4

noteworthy that the peak potential values for other composite electrodes, regardless of the nature of the electrode materials, seem to be more or less similar. Values of the methanol oxidation peak current densities at the scan rate of 50 $mVs^{-1}$, as listed in Table 1, show that the electrocatalytic activity of the Pd-0.5% C electrode is the greatest, while that of the Pt/GC electrode is the lowest one. Based on the anodic oxidation peak current densities, the different electrocatalysts of the present investigation follow the activity order:

$$Pd-0.5\%C > Pd-0.5\%C-1\%Ni > Pd-0.5\%C-2\%Ni > Pd-1\%C > Pd-2\%C > Pd-5\%C > Pd > Pt$$

The observation of Table 1 further shows that 0.5% to 2% C additions to Pd electrode shift the onset potential for MOR in the negative direction, the magnitude in shift, however, being the greatest with 0.5% C. In contrast, introduction of 5%C shifts the onset potential on the base (Pd) electrode towards the noble side by ~20 mV. Furthermore, 1% and 2% Ni additions to Pd-0.5%C composite shift the onset potential of MOR by 80 to 100 mV in the noble direction. Therefore, the onset potential values of the reaction on different electrodes also indicate a higher activity for the Pd-0.5%C composite electrode towards the MOR.

## Impedance spectroscopy

In order to estimate the catalytic film (bulk) resistance, charge transfer resistance for the MOR and double layer capacitance ($C_{dl}$) for the catalytic film/solution interface, the impedance study of some active electrodes, namely, Pd, Pd-0.5%C, Pd-0.5%C-1%Ni, and Pd-0.5%C–2%Ni, has been performed at a constant dc potentials, −0.25 V in 1 M KOH+1 M $CH_3OH$ at 298 K. The chosen potential belongs to the initial region of the MOR. Before recording each impedance spectrum, the electrode was first equilibrated at $E$=−0.25 V for 300 s. The complex impedance diagrams obtained for different electrocatalysts are shown in Fig. 4. Each diagram indicates two arcs, a small arc at high frequencies and a relatively large one at intermediate and low frequencies.

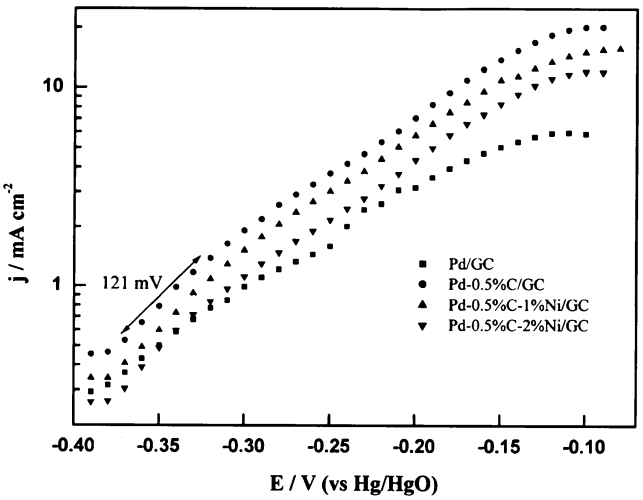


**Fig. 6** Tafel plots for electrocatalysts (scan rate=0.2 mV $s^{-1}$) in 1 M KOH + 1 M $CH_3OH$ at 298 K

In order to fit the experimental impedance data, an equivalent electrical circuit model, $R_s(Q_f(R_f(C_{dl}R_{ct})))$ is proposed, where $R_s$, $R_f$, and $R_{ct}$ are the solution, catalyst film, and charge transfer resistances and $Q_f$ and $C_{dl}$ are the constant phase element and the double layer capacitance for the catalyst mass and catalyst/solution interface, respectively. It is observed that simulated impedance data based on the proposed circuit model agree excellently with those experimentally observed ones. Typical Nyquist plots (simulated + experimental) for Pd-0.5%C-1%Ni electrode are shown in Fig. 5. Estimates of the equivalent circuit parameters are given in Table 2.

Table 2 shows that incorporation of 0.5% C decreases the charge transfer resistance and hence improves the kinetics of methanol electro-oxidation greatly. Further, introduction of 1% Ni to the composite, Pd-0.5%C, does not seem to influence the charge transfer resistance and hence the rate of MOR significantly; however, its higher addition (2%) appears to reduce the rate of MOR considerably. Thus, the results support the findings of the cyclic voltammetry study.

**Table 2** Values of the equivalent circuit parameters of some active electrodes at $E$=−0.25 V in 1 M KOH+1 M $CH_3OH$ at 298 K

| Electrode | Loading (mg $cm^{-2}$) | Rs (Ω $cm^2$) | $10^4$ $Q/F$ $s^{n-1}$ ($cm^{-2}$) | Number | $R_f$ (Ω $cm^2$) | $10^4$ $C_{dl}/F$ ($cm^{-2}$) | $R_{ct}$ (Ω $cm^2$) |
|---|---|---|---|---|---|---|---|
| Pd | 0.18 | 1.71 | 27.21 | 0.58 | 2.02 | 1.04 | 276.1 |
| Pd-0.5%C | 0.15 | 1.35 | 17.09 | 0.68 | 2.20 | 3.63 | 54.9 |
| Pd-0.5%C-1%Ni | 0.15 | 2.66 | 10.96 | 0.78 | 2.16 | 1.31 | 56.0 |
| Pd-0.5%C-2%Ni | 0.14 | 3.28 | 4.92 | 0.85 | 241.3 | 9.14 | 256.1 |

**Table 3** Values of the electrode kinetic parameters for methanol oxidation on pure Pd and active composite electrodes in 1 M KOH+1 M $CH_3OH$ at 298 K

| Electrode | Loading (mg $cm^{-2}$) | EASA (mC $cm^{-2}$ $mg^{-1}$) | Tafel slope, $b$ (mV) | $j$/at $E$/$V$ | | SA (mA $mC^{-1}$) |
|---|---|---|---|---|---|---|
| | | | | −0.20 | | |
| | | | | $j_a$ (mA $cm^{-2}$) | $j_a$ (mA $cm^{-2}$ $mg^{-1}$) | |
| Pd | 0.18 | 42.7 | 145 | 3.20 | 17.78 | 0.42 |
| Pd-0.5%C | 0.15 | 91.8 | 121 | 7.10 | 47.33 | 0.52 |
| Pd-1%C | 0.20 | 28.9 | 120 | 2.32 | 11.62 | 0.40 |
| Pd-2%C | 0.18 | 32.0 | 107 | 3.66 | 20.32 | 0.63 |
| Pd-5%C | 0.19 | 24.4 | 132 | 1.71 | 9.02 | 0.37 |
| Pd-0.5%C-1.0%Ni | 0.15 | 82.6 | 116 | 5.80 | 38.67 | 0.47 |
| Pd-0.5%C-2.0%Ni | 0.14 | 63.2 | 107 | 4.34 | 31.0 | 0.49 |

## Tafel polarization study

The activity test for Pd and composite electrodes has further been carried out by the determination of the IR-compensated quasi-steady-state anodic Tafel polarization curves ($E$ versus $j$) at a slow potential scan rate (0.2 mV $s^{-1}$) in 1 M KOH+1 M $CH_3OH$ at 298 K. Some representative polarization curves for electrocatalysts, namely, Pd, Pd-0.5%C, Pd-0.5%C-1%Ni, and Pd-0.5%C–2%Ni, are given in Fig. 6. The Tafel slope values for the MOR at low potentials were found to be close to 2×2.303 RT/F (i.e., 118±12 mV) on each electrocatalyst, the electrode, Pd/GC ($b$=145 mV), however, being an exception. Based on the apparent current densities ($j_a$) at $E$=−0.20 V (Table 3), the test electrodes followed the activity order: Pd-0.5%C>Pd-0.5%C-1%Ni>Pd-0.5%C–2%Ni>Pd-2%C>Pd>Pd-1%C>Pd-5%C. $j_a$ values were estimated from Fig. 6. The result demonstrates that the performance of the electrode, Pd-0.5%C, is the best among electrodes investigated. Thus, results of the Tafel polarization study more or less corroborate the findings of CV and impedance.

As the activity of an electrode is not only controlled by the catalytic properties but also by the surface area, the electrochemically active surface area (EASA) of the electrodes have been measured by determining the coulombic charge for the reduction of palladium oxide [30]. As shown in Fig. 4, the oxide reduction peak appears at $E$= 296±18 mV on the cyclic voltammograms of electrodes in the background solution (1 M KOH). The coulombic charge ($Q$) for the reduction of palladium oxide has been determined by integrating the oxide reduction peak and is used to calculate the EASA of the electrode. Estimates of $Q$ for different electrodes are shown in Table 3. The specific activities (SA=$j$, mA $cm^{-2}$ $mg^{-1}$/EASA, mC $cm^{-2}$ $mg^{-1}$) of electrodes were also estimated and values are given in Table 3. This table demonstrates that the SA values for the Pd as well as the composite electrodes are practically the same. Thus, the results demonstrates that the introduction of small amount of carbon nanopowder (0.5–5%) does not influence the specific activity of the electrodes. Therefore, the enhanced apparent activity of Pd-0.5%C electrode is mainly due to its improved geometrical properties.

The EASA data shown in Table 3 further show that 0.5%C addition to Pd increases the EASA and hence the porosity greatly, as is also evident from the SEM photographs shown in Fig. 1. However, its higher additions (1–5% C) decrease the EASA significantly. Thus, results demonstrate that in the composite of Pd with 0.5% C, there seems the dispersion of Pd catalyst on nanocarbon particles fairly well, but with the increase in percentage of nanocarbon in the composite, active Pd sites get somehow blocked resulting in the reduced specific surface area. 1% Ni addition to Pd-0.5%C composite does not change the EASA of the electrode significantly. SEM pictures of the composites, Pd-0.5%C and Pd-0.5%C-1%Ni, shown in Fig. 1 also seem to be almost similar. But

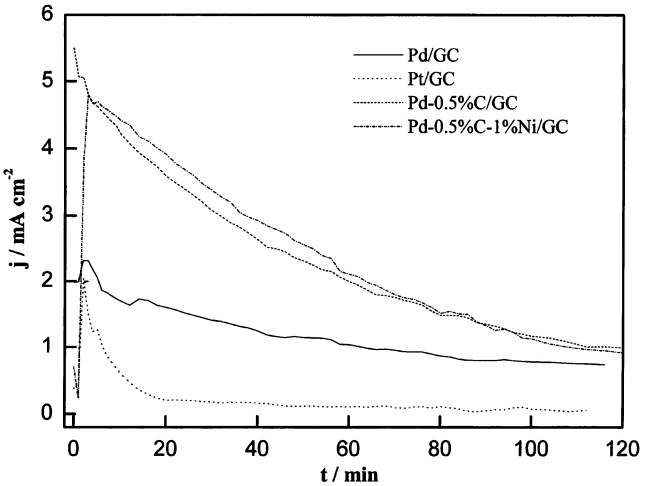


**Fig. 7** Chronoamperograms for Pt, Pd, Pd-0.5%C, and Pd-0.5%C-1% Ni electrodes in 1 M KOH+1 M $CH_3OH$ at 298 K

the higher (2%) or lower (0.5%) addition of Ni than 1% decreased the EASA by 30–70%.

Stability test

The stability of methanol oxidation on Pt/GC, Pd/GC, Pd-0.5%C, and Pd-0.5%C-1%Ni electrodes in 1 M KOH+1 M $CH_3OH$ at 298 K has been investigated by chronoamperometry at $E$=−0.2 V for 2 h. The results are shown in Fig. 7. The rapid current decay shows the poisoning of the electrocatalysts. Values of the apparent current density for methanol oxidation measured after 100 min at $E$=−0.2 V were 1.19, 1.13, 0.79, and 0.07 mA $cm^{-2}$, respectively, on Pd-0.5%C, Pd-0.5%C-1%Ni, Pd, and Pt electrodes. This indicates that Pd-0.5%C electrode is more stable and poisoning-tolerant electrocatalyst compared to conventional Pt electrode in alkaline medium.

## Summary

The study demonstrates that small C addition (0.5%) to Pd greatly improves the apparent catalytic activity and poisoning tolerance, against the methanol oxidation intermediates, of the material. The higher additions of C (1–5%) have been observed to exhibit less beneficial catalytic influence. Introduction of Ni (1–2%) into the Pd-0.5%C composite decreased the apparent electrocatalytic activity of the electrode. The enhanced apparent activity of Pd-0.5%C electrode is mainly due to its improved geometrical properties.

**Acknowledgment** This work was financially supported by the Department of Science and Technology, Government of India through a research project (SR/S1/PC-41).

## References

1. Amphlett JC, Peppley BA, Halliop E, Sadiq A (2001) J Power Sources 96:204. doi:10.1016/S0378-7753(01)00490-6
2. Barragan VM, Heinzel A (2002) J Power Sources 104:66. doi:10.1016/S0378-7753(01)00896-5
3. Ren X, Springer TE, Zawodzmski TA, Gottesfeld S (2000) J Electrochem Soc 147:466. doi:10.1149/1.1393219
4. Scott K, Taama WM, Argyropoulos P, Sundmacher K (1999) J Power Sources 83:204. doi:10.1016/S0378-7753(99)00303-1
5. Zeng J, Lee JY (2007) Int J Hydrogen Energy 32:4389. doi:10.1016/j.ijhydene.2007.03.012
6. Xu C, Shen PK, Ji X, Zeng R, Liu Y (2005) Electrochem Commun 7:1305. doi:10.1016/j.elecom.2005.09.015
7. Wei ZD, Li LL, Luo YH, Yan C, Sun CX, Yin GZ et al (2006) J Phys Chem B 110:26055. doi:10.1021/jp0651891
8. Jafarian M, Moghaddam RB, Mahajani MG, Gobal F (2004) J Appl Electrochem 36:913. doi:10.1007/s10800-006-9155-6
9. Jafarian M, Moghaddam RB, Heli H, Gobal F, Khajehsharifi H, Hamedi MH (2003) Electrochim Acta 48:3423. doi:10.1016/S0013-4686(03)00399-2
10. Cubeiro ML, Fierro JLG (1998) Appl Catal 168:307. doi:10.1016/S0926-860X(97)00361-X
11. Fleischmann M, Korinek K, Pletcher D (1971) J Electroanal Chem 31:39. doi:10.1016/S0022-0728(71)80040-2
12. Heli H, Jafarian M, Mahajani MG, Gobal F (2004) Electrochim Acta 49:4999. doi:10.1016/j.electacta.2004.06.015
13. Xu C, Cheng L, Shen PK, Liu Y (2007) Electrochem Commun 9:997. doi:10.1016/j.elecom.2006.12.003
14. Shen PK, Xu CW (2006) Electrochem Commun 8:184. doi:10.1016/j.elecom.2005.11.013
15. Shen PK, Xu CW, Zeng R (2006) Electrochem Solid-State Lett 9: A39. doi:10.1149/1.2139975
16. Savadogo O, Lee K, Oishi K, Mitsushima S, Kamiya N, Ota K-I (2004) Electrochem Commun 6:105. doi:10.1016/j.elecom.2003.10.020
17. Ha S, Larsen R, Zhu Y, Masel RI (2004) Fuel Cells (Weinh) 4:337. doi:10.1002/fuce.200400052
18. Ha S, Larsen R, Masel RI (2005) J Power Sources 144:28. doi:10.1016/j.jpowsour.2004.12.031
19. Lee C-L (2007) J Solid State Chem 11:1313
20. Lee C-L, Huang Y-C, Kuo L-C, Lin Y-W (2007) Carbon 45:203. doi:10.1016/j.carbon.2006.10.007
21. Wang M, Guo D-J, Li H-L (2005) J Solid State Chem 178:1996. doi:10.1016/j.jssc.2005.04.006
22. Zhang F-B, Li H-L (2006) Carbon 44:3195. doi:10.1016/j.carbon.2006.06.040
23. Zhang K-F, Guo D-J, Liu X, Li J, Li H-L, Su Z-X (2006) J Power Sources 162:1077. doi:10.1016/j.jpowsour.2006.07.042
24. Shen PK, Xu C, Zeng R, Liu Y (2006) Electrochem Solid-State Lett 9(2):A39. doi:10.1149/1.2139975
25. Singh JP, Zhang XG, Li H-L, Singh A, Singh RN (2008) Int J Electrochem Sci 3:416
26. Lal B, Singh NK, Samuel S, Singh RN (1999) J N Mater Electrochem Syst 2:59
27. Huang JC, Liu ZL, He CB, Gan LM (2005) J Phys Chem B 109:16644. doi:10.1021/jp052667j
28. Liu J, Ye J, Xu C, Jiang SP, Tong Y (2007) Electrochem Commun 9:2334. doi:10.1016/j.elecom.2007.06.036
29. Xu M-W, Gao G-Y, Zhou W-J, Zhang K-F, Li H-L (2008) J Power Sources 175:217
30. Pattabiraman R (1997) Appl Catal Gen 153:9. doi:10.1016/S0926-860X(96)00327-4